

© This manuscript version is made available under the CC-BY-NC-ND 4.0 license <https://creativecommons.org/licenses/by-nc-nd/4.0/>

The definitive publisher version is available online at <https://doi.org/10.1016/j.biortech.2023.129384>

New chitosan-biochar composite derived from agricultural waste for removing sulfamethoxazole antibiotics in water

Van Son Tran^a, Huu Hao Ngo^{b,*}, Wenshan Guo^b, Thanh Ha Nguyen^a, Thi Mai Ly Luong^a, Xuan Huan Nguyen^a, Thi Lan Anh Phan^{c,d}, Van Trong Le^{a,e}, Minh Phuong Nguyen^a, Manh Khai Nguyen^a

^a: *Faculty of Environmental Sciences, University of Science, Vietnam National University, Hanoi, 334 Nguyen Trai Road, Thanh Xuan District, Hanoi, Vietnam.*

^b: *Centre for Technology in Water and Wastewater, School of Civil and Environmental Engineering, University of Technology Sydney, Broadway, NSW 2007, Australia.*

^c: *VNU Key Laboratory of Analytical Technology for Environmental Quality and Food Safety Control (KLATEFOS), University of Science, Vietnam National University, Hanoi, 334 Nguyen Trai, Hanoi, Vietnam*

^d: *Research Centre for Environmental Technology and Sustainable Development, University of Science, Vietnam National University, Hanoi, 334 Nguyen Trai Road, Thanh Xuan District, Hanoi, Vietnam.*

^e: *Food Industries Research Institute, Ministry of Industry and Trade, Viet Nam.*

*Corresponding author: Huu Hao Ngo, E-mail: ngohuuhaol21@gmail.com

Abstract

This study aims to develop a new chitosan-biochar composite derived from agricultural waste for removing sulfamethoxazole (SMX) antibiotics in water. Biochar was prepared from orange peel (OB) and spent coffee grounds (SCB). To fabricate chitosan-biochar composites, chitosan and biochar were crosslinked with glutaraldehyde. Results showed that pH, adsorbent dosage, time, temperature, and initial concentrations have a significant impact on the SMX adsorption. The adsorption data was better described by Langmuir (with good regression) than Freundlich model. The highest adsorption capacity (Q_{\max}) of SMX on OB, SCB, CTS-OB, and CTS-SCB were 3.49, 7.65, 7.24, and 14.73 mg/g, respectively. The Freundlich constant (K_F) values for adsorption capacity were 1.66, 1.91, 2.57, and 5.57 ($\text{mg}^{1-n}\text{L}^n/\text{g}$), respectively, for OB, SCB, CTS-OB, and CTS-SCB. Ion exchange, π bonding, hydrogen bonding and pore filling, were proposed as dominant mechanisms of SMX removal process.

Keywords: antibiotic removal, agricultural by-product, glutaraldehyde, cross-linking, chitosan-biochar adsorbent.

1. Introduction

Recently, pharmaceutical compounds are extensively used as human and veterinary medicine to combat diseases (Lu et al., 2016). Nevertheless, the widespread use and continuous release of these chemicals have resulted in increased their concentrations in the environment (Rasoulzade et al., 2019), leading to water contamination, which has become a significant environmental issue (Jia et al., 2016; Rajapaksha et al., 2015). Residues of these substances, especially in water body, do so via release from sources including municipal, medical and agricultural ones (Pouran et al., 2014). Antibiotic remains in water sources can contaminate human food chains, even at low concentrations (Lundborg and Tamhankar, 2017), causing potential hazards of environmental harmfulness and microbial resistance (Lu et al., 2016). Microorganisms have natural adaptations to counteract factors that limit their growth, leading to antimicrobial resistance (Grenni et al., 2018). Currently, all antibiotics used in humans and animals have reported antibiotic resistance, and the existence and occurrence of them in the medium have altered the microorganisms' genetic structure, which could potentially create new pathogens that pose a danger to human health (Martinez, 2009).

Sulfamethoxazole (SMX) belongs to sulfonamide compounds. It is the most stable among the long-lasting environmental sulfonamides, with over 51.7 days of half-life in water and less than 25.6 days in sediments (Danner et al., 2019). SMX can transform into toxic intermediates or accumulate in aquatic organisms when existing in the environment. Acetyl metabolites, such as N4-acetyl sulfamethoxazole, frequently appear in the background and can convert back to SMX (Prasannamedha and Kumar, 2020). SMX antibiotics are commonly used in human and animal medicines due to their low cost and high effectiveness, making SMX one of the most usually identified drug residues in aquatic surroundings worldwide (Lundborg and Tamhankar, 2017). In Europe, it is the second most spent antibiotic in husbandry subsequently tetracycline (Białk-Bielińska et al., 2011). SMX was detected at significant levels in water because of its poor binding capacity in clay (Rajapaksha et al., 2015). In Vietnam, sulfamethoxazole, erythromycin, and amoxicillin existed as the most plentiful pharmaceutical residues in inner-city canals (average levels exceeding 1000 ng/L), while others were frequently found with lower average concentrations (less than 100 ng/L) (Tran et al., 2019). In another report, identified concentrations of sulfamethoxazole; ciprofloxacin; ofloxacin and trimethoprim were 252; 41; 85 and 107 µg/L, consistently in medical producers and other sources nearby Hanoi (Thai et al., 2018). Hoa et al. (2011) reported that during dry season in the north of Vietnam, sulfamethazine was the main pollutant in swine wastewater ponds (its levels varied from 475 to 6662 ng/L), while sulfamethoxazole was the dominant one in city canals (its levels varied from 612 to 4330 ng/L).

To date, many methods, for instance, advanced oxidation processes, biotechnology, adsorption by commercial activated carbon, ion exchange, coagulation and flocculation were utilised for removing antibiotics and supplementary medicines in water (Liu et al., 2021; Heo et al., 2019; Tran et al., 2017). Conversely, the conventional approaches are temperately fruitless to abate the contaminants from aquatic environment (Qiang et al., 2013). Adsorption by low-cost adsorbents can be an operative manner for the elimination of antibiotics from aqueous solution. Using waste constituents to make adsorbents aims to eliminate antibiotic residues from water while minimizing large amounts of solid waste. Agricultural wastes are frequently used to prepare adsorbents due to the lignin and silica content of lignocellulose (Tran et al., 2015).

Adsorbent achieved from agricultural by-products are accessible, low-cost and environmentally friendly. Some agents can use them directly as adsorbents or modify them to improve adsorption efficiency. Waste can be enhanced by physical transformation (pyrolysis) and activated by chemicals such as NaOH, H₃PO₄, HCl, H₂SO₄ methanol, acetone and KMnO₄ (Tran et al., 2015). The keys to eliminating antibiotics by the adsorbents are electrostatic attraction, interaction π , hydrogen bonding and Van Der Waals (Dai et al., 2018). Due to their low-cost, local availability and environmentally friendly, natural polysaccharides (such as chitosan), obtained from biomass waste or by-products, marine resources, and microorganisms, received a lot of attentions (Salehizadeh et al., 2018).

Chitosan is a biopolymer formed through the deacetylation of chitin, a natural mucopolysaccharide originate from the crustaceans' exoskeletons and ranked the second greatest plentiful natural polymer next to lignocellulose (Wang and Chen, 2014). Several reports have investigated eliminating antibiotics from the liquid medium using original and modified chitosan (Long et al., 2019; Liu et al., 2021; Soares et al., 2019). The food processing industry in Vietnam generates tons of by-products, including shrimp or crab shells. Therefore, finding a novel water treatment method, reducing solid waste, and adding more value to the products could help sustainable development in the local area. Furthermore, preparing novel adsorbents such as composites or combined natural polymers for pollutant elimination has received a lot of interest, especially new techniques such as crosslinking chitosan with other suitable organic compounds making mixed more functional groups and more stable in water treatment applications. However, fabricating chitosan combined with other agricultural waste adsorbents (e.g. biochar) and the mechanisms for removing antibiotics from these adsorbents have yet to be detailed mentioned.

This study aims to develop a new chitosan-biochar composite derived from agricultural waste (e.g., orange peel, spent coffee grounds, and shrimp shells) for sulfamethoxazole antibiotics removal in water. This study emphasis on the adsorbents' characteristics, factors affecting antibiotic removal efficiency, adsorption thermodynamic, isotherms and uptake mechanisms.

2. Materials and methods

2.1. Preparation of adsorbent

This study involves the preparation of a chitosan adsorbent from shrimp shells for the removal of an antibiotic stock solution of sulfamethoxazole (SMX) 200 mg/L. The SMX stock solution was concocted using antibiotic powder from Sigma Aldrich Co. and deionized water (SMX-200). Two types of biochar were used in this study: orange biochar (OB) and spent coffee grounds biochar (SCB). The orange peels and spent coffee grounds were taken from native shops in Hanoi and cleaned with distilled water to eradicate impurities. They were then desiccated at 80°C until they reached a constant mass, and milled and sieved to a particle dimension of less than 180 μ m. The particles were then denatured by soaking them in 10% phosphoric acid (H₃PO₄) for 7 hours and desiccated at 100°C until a constant weight. To obtain OB, orange peel was heated in nitrogen from room temperature to 350°C (10°C/min) and retained for 3 hours. To prepare SCB, the same procedures were followed but the material was carbonized at 600°C for 1 hour.

Shrimp shells were collected from seafood stalls in Thanh Xuan Bac market, Thanh Xuan district, Hanoi, Vietnam, and used to extract chitosan. The collected shells were washed and had their legs, eyes, and other protein trash removed. The cleaned shells were then dried at 80°C until they were completely dry. To remove inorganic impurities, proteins, and pigments from the dried shells and obtain chitin, a solution of HCl 10%, NaOH 3%, KMnO₄ 1%, and oxalic acid 1% was used. Chitosan was obtained by deacetylating chitin in a 50% NaOH solution. To prepare the chitosan-biochar composite, OB/SCB and CTS were used, following the procedure shown in Fig. 1. First, CTS flakes and a 2% acetic acid solution (2 grams of flake CTS + 100 mL of acetic acid 2% solution) were combined to obtain CTS gel. Next, OB was added to the obtained chitosan gel at a weight ratio of 1:1 of CTS flake/biochar and stirred well for 30 min. A 3% glutaraldehyde solution was added to create cross-linkages in the materials and stirred until a uniform mixture was obtained and condensed. The resulting product was cut into 5x5 mm sizes and then desiccated at 80°C to get the composite adsorbent CTS-OB. The same process was applied to SCB to form the adsorbent CTS-SCB (Fig. 1).

Fig. 1.

2.2. Characterization of adsorbents

The prepared adsorbents were characterized using several techniques. Scanning Electron Microscopy (SEM) Hitachi TM4000Plus and Fourier Transform Infrared Spectroscopy (FTIR) Nicolet Jasco FT/IR-4600 were utilised to examine the surface's morphology and functional groups. Zeta potential was measured using the PCD5 Particle Charge Detector to determine the electrical charge of the adsorbents. The crystallinity and elementary composition of adsorbents were determined by X-Ray Diffraction (XRD) JSX 1000s and X-ray fluorescence (XRF) Miniflex600. Brunauer, Emmett and Teller (BET) NOVA touch 4LX equipment was used to analyze surface area, pore volume and pore size. These techniques provided valuable information on the properties of the adsorbents and helped to determine their suitability for the intended application.

2.3. Adsorption influencing factors

To determine the most appropriate conditions for SMX abatement, the effects of several factors (pH, dose, contact time, and temperature) were assessed. The effectiveness of SMX removal was measured using the following equation:

$$\% \text{ removal} = \frac{(C_o - C_t) \times 100}{C_o}$$

besides uptake capacity was evaluated using the under formula:

$$Q_e = \frac{(C_o - C_t) \times V}{m}$$

Where C_o and C_t : initial and final (at equilibrium) SMX concentrations (mg/L), m : mass of adsorbent (g) and V (L): volume of the SMX solutions.

The tests were conducted using four different adsorbents (OB, SCB, CTS-OB, and CTS-SCB) separately, following the procedure below:

To explore the effect of pH on SMX adsorption, 100 mL of SMX 5 mg/L was prepared and adjusted to pH 3-9 using 0.1% HCl acid (v/v) and 0.1% NaOH (v/v) in 250 mL flasks. Adding 0.5 g of adsorbent to flasks, then shaken at 150 rpm for 8 hours at room temperature. The effluent was clarified through a 0.22 μm filter paper, collected, and examined by HPLC-UV.

The effects of adsorbent dose (1, 2, 5, 10, and 20 g/L) on the abatement course of antibiotic were investigated. Different quantities of material (0.1, 0.2, 0.5, 1, and 2 g) were put into 100 mL of 5 mg/L SMX solution. The solution pH was changed to the optimal value determined from the overhead experiments. The consequent stages were conducted succeeding the similar practice as the pH affecting examinations.

The effect of contact time was examined by preparing 1000 mL of SMX 5 mg/L solution in a 2000 mL beaker with the best pH and dose. The mix was vibrated at 150 rpm, and effluent were sampled after 5, 10, 15, 30, 60, 90, 120, 150, 180, 210, 240, 270, 300, 330, 360, 390, 420, and 480 min. Samples were filtered and analyzed using the same procedure as above experiments.

The effect of temperature on elimination performance was experimented at 20, 25, and 30 $^{\circ}\text{C}$ using 100 mL of SMX 5 mg/L put into 250 mL bottles with the optimum pH and dosage. The mixtures were vibrated at 150 rpm in a thermostatic vibrater in the optimum time duration. Succeeding steps were conducted as the pH influence practice. The temperature effect on the adsorption performance of SMX by the materials was investigated, and the thermodynamic factors were determined using Van't Hoff and Arrhenius equations (Tran et al., 2017). The distribution coefficient of SMX adsorption proficiencies, K_d , was decided at a specific temperature by plotting $\ln(q_e/C_e)$ versus q_e , and Gibbs free energy (ΔG°), enthalpy (ΔH°), and entropy (ΔS°) were defined utilising Eqs. 1 and 2.

$$\Delta G^{\circ} = -RT \ln K_d \text{ (Eq. 1)}$$

$$\ln K_d = \frac{-\Delta H^{\circ}}{RT} + \frac{\Delta S^{\circ}}{R} \text{ (Eq. 2)}$$

2.4. SMX adsorption isotherms

sotherm models, including Langmuir and Freundlich, were employed to designate SMX adsorption onto studied adsorbents (equations and linearized formulas of the simulations are concised in the supplementary material).

The adsorption isothermal experiment was carried out separately for four types of adsorbents according to the following procedure: 100 mL solutions of SMX at different concentrations (3, 5, 10, 20, 50, 75 mg/L) were set in 250 mL bottles. The optimal pH, dosage, temperature was adjusted, and mixtures were shaken at 150 rpm for a duration of 24 hours. Subsequently, filtrates were passed via a 0.22 μm filter, and SMX concentration was analyzed using HPLC-UV.

2.5. Analytical methods

Concentration of antibiotic in the experiment samples was determined using the Shimadzu LC-20A liquid chromatograph system, which was connected to a UV/Vis SPD-20A detector at 285 nm, using an ODS C18 column. The mobile phase comprised of two solutions, A and B, with a 50/50 ratio (v/v). Solution A consisted of a mix of acetonitrile and phosphoric acid with 99.9: 0.1 ratio (v/v), while solution B comprised of deionized water and phosphoric acid with a ratio of (v/v) 99.9: 0.1. The analysis running time and the SMX' retention time were 10 and 5.77 min. Standard solutions were prepared from a stock solution to reach concentrations of 1, 2, 5, and 10 mg/L, with a regression value of $R^2 = 0.9998$ (see supplementary material).

3. Results and discussion

3.1. Adsorbents' surface characteristics

The SEM images (see supplementary material) show that surface structures of the adsorbents are heterogeneous. The surface of chitosan derived from shrimp shells has flat, condensed, and smooth morphology, while the adsorbents exhibit numerous holes and large grooves with different sizes, which is similar to preceding reports (Li et al., 2013). These surface features indicate that the materials might be effective adsorbents. However, the biochar-only adsorbents (OB and SCB) contain more pores than the composite materials (CTS-OB and CTS-SCB). This could be elucidated that the formation of composites lowers surface area and number of pores in the materials. Additionally, cross-linkages were created in the composite structure by glutaraldehyde, which impacts the bulk and form of the resulting glutaraldehyde-crosslinked chitosan. The degree of cross-linking and deacetylation are known to affect the bulk and morphology of the material (Li et al., 2013). Furthermore, the biochar in the composites makes their surface morphology different from that of glutaraldehyde-crosslinked chitosan in other studies. The porous structure of the composites could provide extra adsorption positions for the pollutant in water.

FTIR results indicate that the surface of the adsorbents contains functional groups from biochar that can be assigned as follows: the 3600 cm^{-1} peak shifts to 3300 cm^{-1} (-OH and -NH stretching vibration), and the 1640 cm^{-1} peak shifts to 1546 cm^{-1} for C=C, C=O, and C-O stretching vibration (see supplementary material). Additionally, the IR spectrum of CTS-adsorbents contains stretching vibrations for chitosan, such as C-N at 1379 cm^{-1} and C-O-C bending vibration at 1070 cm^{-1} . Notably, the 1650 cm^{-1} peak for C=N stretching vibration is a result of the cross-linking reaction between CTS and glutaraldehyde. Li et al. (2013) reported that the cross-linkage between chitosan and glutaraldehyde is present at 1559 cm^{-1} . In other studies, Jawad et al. (2021) reported a C=N stretching vibration at 1650 cm^{-1} , while Chang et al. (2008) suggested that the C=N stretching vibration of cross-linkage of chitosan appears at $1653\text{--}1656\text{ cm}^{-1}$.

The zeta potential (mV) values presented in Fig. 2 indicate that OB and SCB biochar exhibit a negative charge on their surface in the pH range studied. These findings are consistent with typical characteristics of biochar and are supported by earlier studies. As Ahsan et al. (2018) stated that adsorbents derived from the sulfonation process of spent coffee grounds also exhibit a negative charge on their surface. Similarly, Pandiarajan et al. (2018) demonstrated that

activated carbon prepared from orange peel exhibits a negative charge in alkaline conditions and switches to a positive charge in acidic medium. In contrast, the CTS-OB and CTS-SCB composites exhibit a positive charge in the pH range of 3 to 9. This finding is in agreement with a research done by Chang et al. (2008) that confirmed positive charges of cross-linked chitosan aerogels at pH values below 9. Moreover, zeta-potential studies of chitosan-glutaraldehyde aerogels have revealed that pH_{pzc} of these materials is approximately 9.5 (Poon et al., 2014). Therefore, the positively charged surface of the composites in this study in the pH range of 3 to 9 is reasonable. The FTIR and Zeta potential results indicate differences between composite materials and precursor biochar, demonstrating changes in surface properties after cross-linking. These changes can potentially enhance or contribute to adsorption progression.

Fig. 2.

XRD patterns of the biochars and composites in this study (see supplementary material) exhibited a broad peak at $2\theta = 24^\circ$, indicating that the adsorbents possess a crystalline structure. In contrast, Zhang et al. (2020) reported that biochar and hydrochar originate from used coffee powder have a graphite-like structure. Furthermore, Pandiarajan et al. (2018) observed two weak peaks at $2\theta = 43.47^\circ$ and 23.38° on the surface of activated carbon made of orange peel then concluded that activated carbon's surface structure is amorphous.

Regarding the cross-linked chitosan, Li et al. (2013) used the XRD method to investigate the modifications in the building of chitosan subsequently cross-linking with glutaraldehyde. They found that diffraction peaks at $2\theta = 10^\circ$ and 20° vanished, and a weak peak was seen at $2\theta = 15^\circ$, indicating the effects of the cross-linking process. This could be explained by the replacement of hydroxyl and amino groups, causing deformation of hydrogen bond on chitosan's surface and forming amorphous structure (Li et al., 2013).

The elemental composition analysis of the adsorbents (OB, SCB, CTS-OB, and CTS-SCB) revealed differences in composition. The primary elemental components (more than 1% of weight percentage, in descending order) of each material were (OB: C, O, N, H, P, Ca, K, Si, Al; SCB: C, O, N, H, Ca, P, K, Si, Fe, Al, S, Cu; CTS-OB: C, O, H, N, P, Si, Ca, K, Al; CTS-SCB: C, O, H, N, Si, P, Ca, K, Al, Fe, S, Cu). These findings are consistent with previous reports indicating that C, O, N, and H are primary components of biochars derived from spent coffee grounds (Zhang et al., 2020), sunflower seed husk (Nguyen et al., 2023) and that chitosan and cross-linked chitosan-glutaraldehyde have dominant compositions of C, H, and N (Li et al. 2013).

The BET outcomes revealed that surface areas (m^2/g) of chitosan, OB, SCB, CTS-OB, and CTS-SCB were 0.35, 1.36, 2.16, 1.29, and 1.78, respectively. The results suggest that the formation of composites between chitosan and glutaraldehyde reduced the surface area and the number of pores in CTS-OB and CTS-SCB, as evidenced by the SEM images. Moreover, the pore volume and pore radius of SCB ($0.005847 \text{ cm}^3/\text{g}$ and 2.83 nm) decreased to $0.002972 \text{ cm}^3/\text{g}$ and 1.53 nm , respectively, for CTS-SCB. While the BET surface area and pore bulk of materials in present study are higher than those informed by Zhang et al. (2020) for biochar obtained from used coffee grounds, adsorbent pore radius is smaller.

3.2. Effect of pH

Adsorption of SMX onto studied materials was significantly influenced by the solution pH (Fig. 3a). The speciation of sulfonamide groups results in the dominance of anionic, neutral, and cationic species of sulfamethazine at alkaline pH, neutral pH, and $\text{pH} < 2.5$, correspondingly (Tran et al., 2017). Experimental results revealed that the cross-linked chitosan/biochar composites had higher adsorption capacities for SMX than the original biochar. Results indicate that more functional groups were created by cross-linking chitosan with glutaraldehyde, as evidenced by the FTIR spectra. Maximum uptake capabilities of SMX onto the materials were achieved at pH 5 and pH 7. At pH 5, adsorption proficiencies of SMX onto OB, SCB, CTS-OB, and CTS-SCB were 0.999, 2.868, 2.602, and 4.179 mg/g, respectively. The surface charge of SMX is neutral at pH 2 to 5.7, resulting in low electrical repulsion and promoting the adsorption process. Another study proposed that a hydrogen bond is formed between neutral SMX and the amino and hydroxyl groups on the surface of adsorbent (Eniola et al., 2019). π - π interaction is also suggested as a mechanism for SMX adsorption onto adsorbents, where double bonds such as C=C, C=O on the materials' surface interact with antibiotics by π - π interaction (Ahsan et al., 2018).

The second maximum binding volume was reached by pH 7 when the charge of SMX' surface changed to negative. Surface charge of composite materials (CTS-OB and CTS-SCB) is positive (Fig. 2), enhancing the adsorption capacities of the composite materials through electrical interactions (formation of hydrogen bonding) (Fan et al., 2012). As revealed in the Zeta potential section, cross-linking with glutaraldehyde altered the surface charge of the material, changing it from negative in biochar to positive in chitosan-biochar composites. At pH 7, SMX binding capacities onto CTS-OB and CTS-SCB were 2.946 and 4.227 mg/g, respectively. The two biochar materials also had high adsorption capacities at pH 7, which were 1.020 and 3.174 mg/g, respectively.

The optimal pH for the adsorption process is neutral. Therefore, the use of the materials in this study does not require any chemicals to adjust the solution pH. Compared with SMX adsorbent materials derived from by-products such as denatured steel materials reported by Tran et al. (2017), the SMX adsorption efficiency achieved at pH 2.5-2.9 is 93.6% at an initial concentration of SMX of 1 ppm and an adsorbent dose of 10 g/L. Other authors have also demonstrated that materials produced from spent coffee grounds modified with H_2SO_4 treat SMX well at low pH (Ahsan et al., 2018). Similarly, Soares et al. (2019) specified that Fe_3O_4 -coated Fe_3O_4 material showed high adsorption of antibiotics at pH 5.

3.3. Adsorbent dose effect

Effects of adsorbent dosage on antibiotics binding is illustrated in Fig. 3b. Since the adsorbent dose enlarged from 1 to 20 g/L, better adsorption efficiencies were achieved, while the adsorption capacity decreased. This can be due to the increase in adsorbent dosage leading to more active sites available for SMX binding on the surface. However, Fig. 3b showed that the SMX adsorption capacity by the adsorbents declines with growing biosorbent dose till a certain value. This is due to the agglomeration phenomenon that occurs with higher dosages, reducing the overall active surface area and therefore rising the diffusion (Ahsan et al., 2018).

Based on the uptake effectiveness and adsorption volumes, a 2 g/L dose was chosen intended for subsequent experiments. The abatement efficiencies achieved with this dosage were 83.0; 90.9; 88.4 and 99.4% for OB; SCB; CTS-OB; and CTS-SCB, respectively. The corresponding adsorption capacities were 2.076, 2.273, 2.210, and 2.485 mg/L.

3.4. Effect of time

In Fig. 3c, it can be observed that the adsorption of SMX antibiotics by the adsorbents was rapid within first 90 min. At 90 min, the adsorption efficiencies were 87.64 and 90.1% with corresponding adsorption bulks of 1.018 and 2.391 mg/g for OB and SCB, respectively. OB and SCB reached equilibrium at 120 min. In contrast, the SMX adsorption process for the composite materials (CTS-OB, CTS-SCB) took longer than that for the biochar materials (OB and SCB). The highest adsorption capacities for CTS-OB and CTS-SCB were achieved after 360 and 390 min, respectively, with uptake capabilities of 2.438 and 4.480 mg/g, separately. From above results, 90 min contact time was chosen for investigations regarding effect of temperature/thermodynamic. These results agreed with previous studies. For example, Ahsan et al. (2018) applied biochar from coffee grounds, and SMX adsorption reached equilibrium within the first 30 min. In another study, Soares et al. (2019) tested the SMX adsorption process of Fe₃O₄@SiO₂/SiCHIT composite materials. They found that the uptake bulk rose with rising initial SMX levels, and the binding process occurred rapidly within a short contact time of 15 min. Experimental results revealed that the adsorbents in this study also quickly worked in the first mins (0 – 90 min), but it took longer than other prior materials to reach equilibrium.

3.5. Effect of temperature/thermodynamic

From experimental data, it was found that the temperature important influenced on SMX binding process by the materials. The adsorbents displayed the highest adsorption abilities for SMX at 25°C, with amounts of 1.040, 2.126, 2.155, and 4.504 mg/g for OB, SCB, CTS-OB, and CTS-SCB materials, respectively (Fig. 3d). Thermodynamic factors for binding performance are briefly described in Table 1. Negative values of ΔG directed that the abatement of SMX on biochar and composite materials is naturally spontaneous. The category of adsorption progression can be described depending on the ΔG values, where values among 0 and 20 kJ/mol specify predominantly physical adsorption and values varied from 80 to 400 kJ/mol is chemical binding process (Ahsan et al., 2018). The obtained ΔG values were in the range of 908 – 8004 J/mol or 0.9–8.0 kJ/mol, indicating physical adsorption progression is dominant. Similar outcomes were achieved for removal of sulfamethoxazole and bisphenol A by means of CuZnFe₂O₄-biochar composite. The high values of positive ΔS° exhibit growing uncertainty at the solid-liquid interface of CTS-OB and CTS-SCB (Heo et al., 2019).

The SMX binding onto biochar (OB and SCB) was found to be exothermic due to the negative ΔH values. In contrast, the SMX adsorption onto the composite materials (CTS-OB and CTS-SCB) was endothermic due to the positive ΔH values. However, the adsorption process achieved the highest capacities at 25°C. Thus 25°C is enough and the most suitable temperature for the adsorption process. This temperature is average room temperature. Hence, it has practical significance. Therefore, the adsorption isotherm tests were conducted at a temperature of 25°C.

Fig. 3.

Table 1.

3.6. Modeling of sorption isotherms

The results of the adsorption isotherms based on Langmuir, Freundlich simulations are presented in Fig. 4 and Table 2. Adsorption capacities of antibiotics enlarged as the original concentrations increased. The SMX adsorption performance was better depicted by Langmuir than Freundlich model, with good regression values ($0.9992 \leq R^2 \leq 0.9997$). The supreme Langmuir adsorption capacities (Q_{\max} mg/g) for OB, SCB, CTS-OB, and CTS-SCB were 3.49, 7.65, 7.24, and 14.73 mg/g, separately. The arrangement of SMX's sorption capability on the materials was $OB < CTS-OB < SCB < CTS-SCB$. The experimental outcomes indicated that the composite preparation process using chitosan and cross-linking substance (glutaraldehyde) successfully enhanced the adsorption capacities of materials compared to original biochars. The uptake volumes of SMX adsorption onto composite materials were nearly two-fold higher than biochar. The Freundlich model had smaller R^2 regressions and lower adsorption capacity (KF) values of 1.66, 1.91, 2.57, and 5.57 ($\text{mg}^{1-n}\text{L}^n/\text{g}$), respectively, for SMT adsorption on OB, SCB, CTS-OB, and CTS-SCB. Here, n is Freundlich constant representing the adsorption strength of the materials. The investigated adsorbents had values much greater than 1, indicating that the surface of the material is not uniform, which is favorable for the adsorption process (Pandiarajan et al., 2018).

The inspected adsorbents in the present study had higher adsorption aptitudes than conveyed values in prior studies that used dissimilar adsorbents, including biochar, hydrochar, or composite chitosan-biochar, for removing SMX in water. For instance, Zhang et al. (2020) reported both Langmuir and Freundlich simulations are suitable for SMX adsorption of biochar and hydrochar materials derived from coffee grounds. The Langmuir Q_{\max} values were 740.6 and 481.6 $\mu\text{g/g}$ for hydrochar and biochar, respectively. The Freundlich constant n was less than 1 in both cases. Meanwhile, the chitosan and biochar composites reported by Jawad et al. (2021) were consistent with the Freundlich isotherm, with a K_F value of 1.9 $\text{mg}^{1-n}\text{L}^n/\text{g}$ at 323 K.

Fig. 4.**Table 2.**

3.7. Proposed SMX elimination mechanisms

The binding of SMX onto the material can be explained by four main mechanisms: molecular diffusion to the adsorbent's surface (pore filling); electrostatic interactions between antibiotics and material (ion exchange); interactions between the surface of the material rich in polar π -electrons (π - π bonding); and the forming of hydrogen bonds between SMX and O-containing functional groups of the material (hydrogen bonding) (Fig. 5).

The π - π bond contributes a critical part in the uptake mechanism of SMX molecules. Due to their benzene rings and amine groups, antibiotic molecules are capable of accepting π -electrons. On the other hand, the surface of chitosan, biochar and chitosan-biochar materials contains functional groups that can give strong π -electrons such as C=C and C=O, especially C=N in chitosan-biochar composite formed by cross-linkage process as showed in FTIR

spectrums. Therefore, ring π -electron interaction between SMX and double bonds on the surface of the adsorbent forms by π - π electron coupling (Liu et al., 2021; Ahsan et al., 2018).

In present study, at $\text{pH} > 5.7$, the SMX antibiotic carries a negative charge, while the biochar surface is always negatively charged. As a result, the π -electron interaction should be destabilized due to charge repulsion. However, biochar can still adsorb antibiotics through hydrogen bond formation (Heo et al., 2019). In contrast, cross-linking between chitosan and glutaraldehyde leads to a positive surface charge of chitosan-biochar composites, thereby enhancing elimination performance on the composites' surface (see the Zeta potential results). Negative antibiotic molecules release $-\text{OH}$ through proton exchange, which combines with functional groups on the adsorbents' surface (Eniola et al., 2019; Ahmed et al., 2017). In another report, Pamphile et al. (2019) stated that the sulphonamide adsorption process to carbon adsorbents is governed by mechanisms comprising electrostatic and non-electrostatic exchanges, diffusive interaction between π - π electro-donor acceptor, and the pore texture.

Jawad et al. (2021), in a study on using composite of chitosan-glutaraldehyde and activated carbon to remove cationic dye, specified that the adsorption mechanisms comprise electrostatic attraction with negatively functional groups on the composite's surface. Hydrogen bonds between the donor hydrogen sites of the material with O and N of the pollutant also occurs. Additionally, π - π and cation- π interactions happen between the hexagonal skeleton of the composite and the aromatic ring of the pollutant. Thermodynamic analysis conducted in this study suggests that physical processes, such as pore filling, also surplus a vital part in the adsorption of SMX onto the adsorbents. This is also confirmed by SEM images for the surface morphology of the adsorbents and BET surface area and pore volume. This mechanism was also noted by Ahsan et al. (2018) for the removal of sulfamethoxazole and bisphenol A by sulfonated coffee grounds.

This study only investigated the removal of SMX onto biochar and composite adsorbents in synthesized wastewater. Thus, the effects of other substances in natural sewage, such as humic acid, suspended solids, and other ions, were still not mentioned. Further study on preliminary estimation of costs and regeneration of adsorbed materials with different types of reagents needs to be considered to apply this adsorbent for antibiotic elimination in natural wastewater treatment.

Fig. 5.

4. Conclusions

Chitosan-biochar composites were successfully prepared from agricultural waste, including spent coffee grounds, orange peel, and shrimp shells, by loading biochar with chitosan-gel biopolymer and crosslinking with glutaraldehyde. The most suitable conditions for SMX exclusion were observed at $\text{pH} 7$, an adsorbent dose of 2 g/L , a contact time of 90 min , and at 25°C . Cross-linking by means of glutaraldehyde enhanced the adsorption bulk of the chitosan-biochar composite compared to the precursor biochar. This study has significant scientific and practical value in creating an environmentally friendly material for water treatment, reducing waste and promoting a circular economy.

E-supplementary data for this work can be found in e-version of this paper online.

Acknowledgements

This research is funded by Vietnam National Foundation for Science and Technology Development (NAFOSTED) under grant number 105.08-2019.321.

"As Huu Hao Ngo, a [co-]author on this paper, is an editor of Bioresource Technology, he was blinded to this paper during review, and the paper was independently handled by Samir Kumar Khanal as editor."

References

1. Ahmed, M. B., Zhou, J. L., Ngo, H. H., Guo, W., Johir, M. A. H., Sornalingam, K., 2017. Single and competitive sorption properties and mechanism of functionalized biochar for removing sulfonamide antibiotics from water. *Chem. Eng. J.* 311, 348-358.
2. Ahsan, M. A., Islam, M. T., Imam, M. A., Hyder, A. G., Jabbari, V., Dominguez, N., Noveron, J. C., 2018. Biosorption of bisphenol A and sulfamethoxazole from water using sulfonated coffee waste: Isotherm, kinetic and thermodynamic studies. *J. Environ. Chem. Eng.* 6(5), 6602-6611.
3. Białk-Bielińska, A., Stolte, S., Arning, J., Uebers, U., Bösch, A., Stepnowski, P., Matzke, M., 2011. Ecotoxicity evaluation of selected sulfonamides. *Chemosphere.* 85(6), 928-933.
4. Chang, X., Chen, D., Jiao, X., 2008. Chitosan-based aerogels with high adsorption performance. *J. Phys. Chem. B.* 112(26), 7721-7725.
5. Dai, Y., Sun, Q., Wang, W., Lu, L., Liu, M., Li, J., Zheng, W., 2018. Utilizations of agricultural waste as adsorbent for the removal of contaminants: A review. *Chemosphere.* 211, 235-253.
6. Danner, M. C., Robertson, A., Behrends, V., Reiss, J., 2019. Antibiotic pollution in surface fresh waters: occurrence and effects. *Sci. Total Environ.* 664, 793-804.
7. Eniola, J. O., Kumar, R., Barakat, M. A., 2019. Adsorptive removal of antibiotics from water over natural and modified adsorbents. *Environ. Sci. Pollut. Res.* 26, 34775-34788.
8. Fan, L., Luo, C., Sun, M., Li, X., Lu, F., Qiu, H., 2012. Preparation of novel magnetic chitosan/graphene oxide composite as effective adsorbents toward methylene blue. *Bioresour. Technol.* 114, 703-706.
9. Grenni, P., Ancona, V., Caracciolo, A. B., 2018. Ecological effects of antibiotics on natural ecosystems: A review. *Microchem. J.* 136, 25-39.
10. Heo, J., Yoon, Y., Lee, G., Kim, Y., Han, J., Park, C.M., 2019. Enhanced adsorption of bisphenol A and sulfamethoxazole by a novel magnetic CuZnFe₂O₄-biochar composite. *Bioresour. Technol.* 281, 179-187.

11. Hoa, P.T.P., Managaki, S., Nakada, N., Takada, H., Shimizu, A., Anh, D.H., Viet, P.H., Suzuki, S., 2011. Antibiotic contamination and occurrence of antibiotic-resistant bacteria in aquatic environments of northern Vietnam. *Sci. Total Environ.* 409(15), 2894-2901.
12. Jawad, A. H., Abdulhameed, A. S., Wilson, L. D., Hanafiah, M. A. K. M., Nawawi, W. I., ALOthman, Z. A., Rizwan Khan, M., 2021. Fabrication of schiff's base chitosan-glutaraldehyde/activated charcoal composite for cationic dye removal: optimization using response surface methodology. *J. Polym. Environ.* 29(9), 2855-2868.
13. Jia, S., Yang, Z., Ren, K., Tian, Z., Dong, C., Ma, R., Yu, G., Yang, W., 2016. Removal of antibiotics from water in the coexistence of suspended particles and natural organic matters using amino-acid-modified-chitosan flocculants: a combined experimental and theoretical study. *J. Hazard. Mater.* 317, 593-601.
14. Li, B., Shan, C. L., Zhou, Q., Fang, Y., Wang, Y. L., Xu, F., Han, L. R., Ibrahim, M., Gou, L. B., Xie, G. L., Sun, G. C., 2013. Synthesis, characterization, and antibacterial activity of cross-linked chitosan-glutaraldehyde. *Mar. Drugs.* 11(5), 1534-1552.
15. Liu, Y., Nie, P., Yu, F., 2021. Enhanced adsorption of sulfonamides by a novel carboxymethyl cellulose and chitosan-based composite with sulfonated graphene oxide. *Bioresour. Technol.* 320, 124373.
16. Long, L., Hu, X., Yan, J., Zeng, Y., Zhang, J., Xue, Y., 2019. Novel chitosan–ethylene glycol hydrogel for the removal of aqueous perfluorooctanoic acid. *J. Environ. Sci.* 84, 21-28.
17. Lu, H., Zou, W., Chai, P., Wang, J., Bazinet, L., 2016. Feasibility of antibiotic and sulfate ions separation from wastewater using electrodialysis with ultrafiltration membrane. *J. Cleaner Prod.* 112, 3097-3105.
18. Lundborg, C. S., Tamhankar, A. J., 2017. Antibiotic residues in the environment of South East Asia. *Bmj.* 358, 2440.
19. Martinez, J. L., 2009. Environmental pollution by antibiotics and by antibiotic resistance determinants. *Environ. Pollut.* 157(11), 2893-2902.
20. Nguyen, T.B., Chen, W.H., Chen, C.W., Patel, A.K., Bui, X.T., Chen, L., Singhania, R.R., Dong, C.D., 2023. Phosphoric acid-activated biochar derived from sunflower seed husk: selective antibiotic adsorption behavior and mechanism. *Bioresour. Technol.* 128593.
21. Pamphile, N., Xuejiao, L., Guangwei, Y., Yin, W., 2019. Synthesis of a novel core-shell-structure activated carbon material and its application in sulfamethoxazole adsorption. *J. Hazard. Mater.* 368, 602-612.
22. Pandiarajan, A., Kamaraj, R., Vasudevan, S., Vasudevan, S., 2018. OPAC (orange peel activated carbon) derived from waste orange peel for the adsorption of chlorophenoxyacetic acid herbicides from water: adsorption isotherm, kinetic modelling and thermodynamic studies. *Bioresour. Technol.* 261, 329-341.
23. Poon, L., Wilson, L. D., Headley, J. V., 2014. Chitosan-glutaraldehyde copolymers and their sorption properties. *Carbohydr. Polym.* 109, 92-101.

24. Pouran, S.R., Raman, A.A.A., Daud, W.M.A.W., 2014. Review on the application of modified iron oxides as heterogeneous catalysts in Fenton reactions. *J. Cleaner Prod.* 64, 24-35.
25. Prasannamedha, G., Kumar, P. S., 2020. A review on contamination and removal of sulfamethoxazole from aqueous solution using cleaner techniques: Present and future perspective. *J. Cleaner Prod.* 250, 119553.
26. Qiang, Z., Bao, X., Ben, W., 2013. MCM-48 modified magnetic mesoporous nanocomposite as an attractive adsorbent for the removal of sulfamethazine from water. *Water Res.* 47(12), 4107-4114.
27. Rajapaksha, A.U., Vithanage, M., Ahmad, M., Seo, D.C., Cho, J.S., Lee, S.E., Lee, S.S., Ok, Y.S., 2015. Enhanced sulfamethazine removal by steam-activated invasive plant-derived biochar. *J. Hazard. Mater.* 290, 43-50.
28. Rasoulzadeh, H., Mohseni-Bandpei, A., Hosseini, M., Safari, M., 2019. Mechanistic investigation of ciprofloxacin recovery by magnetite-imprinted chitosan nanocomposite: Isotherm, kinetic, thermodynamic and reusability studies. *Int. J. Biol. Macromol.* 133, 712-721.
29. Salehizadeh, H., Yan, N., Farnood, R., 2018. Recent advances in polysaccharide bio-based flocculants. *Biotechnol. Adv.* 36(1), pp.92-119.
30. Soares, S. F., Fernandes, T., Trindade, T., Daniel-da-Silva, A. L., 2019. Trimethyl chitosan/siloxane-hybrid coated Fe₃O₄ nanoparticles for the uptake of sulfamethoxazole from water. *Molecules.* 24(10), 1958.
31. Thai, P.K., Binh, V.N., Nhung, P.H., Nhan, P.T., Hieu, N.Q., Dang, N.T., Tam, N.K.B., Anh, N.T.K., 2018. Occurrence of antibiotic residues and antibiotic-resistant bacteria in effluents of pharmaceutical manufacturers and other sources around Hanoi, Vietnam. *Sci. Total Environ.* 645, 393-400.
32. Tran, N. H., Hoang, L., Nghiem, L. D., Nguyen, N. M. H., Ngo, H. H., Guo, W., Ta, T. T., 2019. Occurrence and risk assessment of multiple classes of antibiotics in urban canals and lakes in Hanoi, Vietnam. *Sci. Total Environ.* 692, 157-174.
33. Tran, V. S., Ngo, H. H., Guo, W., Ton-That, C., Li, J., Li, J., Liu, Y., 2017. Removal of antibiotics (sulfamethazine, tetracycline and chloramphenicol) from aqueous solution by raw and nitrogen plasma modified steel shavings. *Sci. Total Environ.* 601, 845-856.
34. Tran, V. S., Ngo, H. H., Guo, W., Zhang, J., Liang, S., Ton-That, C., Zhang, X., 2015. Typical low cost biosorbents for adsorptive removal of specific organic pollutants from water. *Bioresour. Technol.* 182, 353-363.
35. Wang, J., Chen, C., 2014. Chitosan-based biosorbents: modification and application for biosorption of heavy metals and radionuclides. *Bioresour. Technol.* 160, 129-141.
36. Zhang, X., Zhang, Y., Ngo, H. H., Guo, W., Wen, H., Zhang, D., Qi, L., 2020. Characterization and sulfonamide antibiotics adsorption capacity of spent coffee grounds based biochar and hydrochar. *Sci. Total Environ.* 716, 137015.

Figure Captions

Fig. 1. Procedure for chitosan-biochar composite preparation

Fig. 2. Zeta potential of adsorbents as a function of pH solution:
(a) OB; (b) SCB; (c) CTS-OB; (d) CTS-SCB

Fig. 3. Affecting factors to adsorption process of sulfamethoxazole: (a) pH; (b) adsorbent dosage; (c) contact time; (d) temperature

Fig. 4. Langmuir and Freundlich adsorption of sulfamethoxazole on adsorbents
(pH 7, C_0 : 3 - 75 mg/L; contact time: 24 hours; adsorbent dose: 2g/L; at 25 °C)

Fig. 5. Proposed antibiotics removal mechanisms on the chitosan-biochar composites

TABLES AND FIGURES

TABLES

Table 1

Thermodynamic parameters for SMX sorption on adsorbents

Adsorbent	Temperature (°C)	Q_{\max} exp. (mg/g)	K_d	ΔG° (J/mol)	ΔH° (J/mol)	ΔS° (J/mol/K)	R^2
OB	20	0.958	1.452	-908.655	-98.488	1.097	0.0166
	25	1.040	4.409	-3675.845			
	30	1.042	0.663	-			
SCB	20	1.569	4.370	-3592.581	-288.421	-1.632	0.8158
	25	2.126	3.857	-3344.577			
	30	1.587	2.375	-2178.733			
CTS-OB	20	2.020	0.810	-	584.216	27.542	0.6447
	25	2.155	3.863	-			

	30	2.074	3.566	-3203.161			
	20	4.187	18.47 6	-	1665.045	85.917	0.852 4
CTS-SCB	25	4.504	22.77 0	-7743.512			
	30	4.304	23.98 7	-8004.604			

Table 2

Isotherm parameters utilizing the non-linear regression method for SMX adsorption onto adsorbents

Isotherm parameters	OB	SCB	CTS-OB	CTS-SCB
1. Freundlich				
R ²	0.5886	0.8722	0.6600	0.7578
n	4.29	2.68	3.42	3.57
K _F (mg ¹⁻ⁿ L ⁿ /g)	1.66	1.91	2.57	5.57
2. Langmuir				
R ²	0.9997	0.9996	0.9992	0.9997
Q _{max} (mg/g)	3.49	7.65	7.24	14.73
K _L (L/mg)	0.34	0.28	0.61	0.81

FIGURES

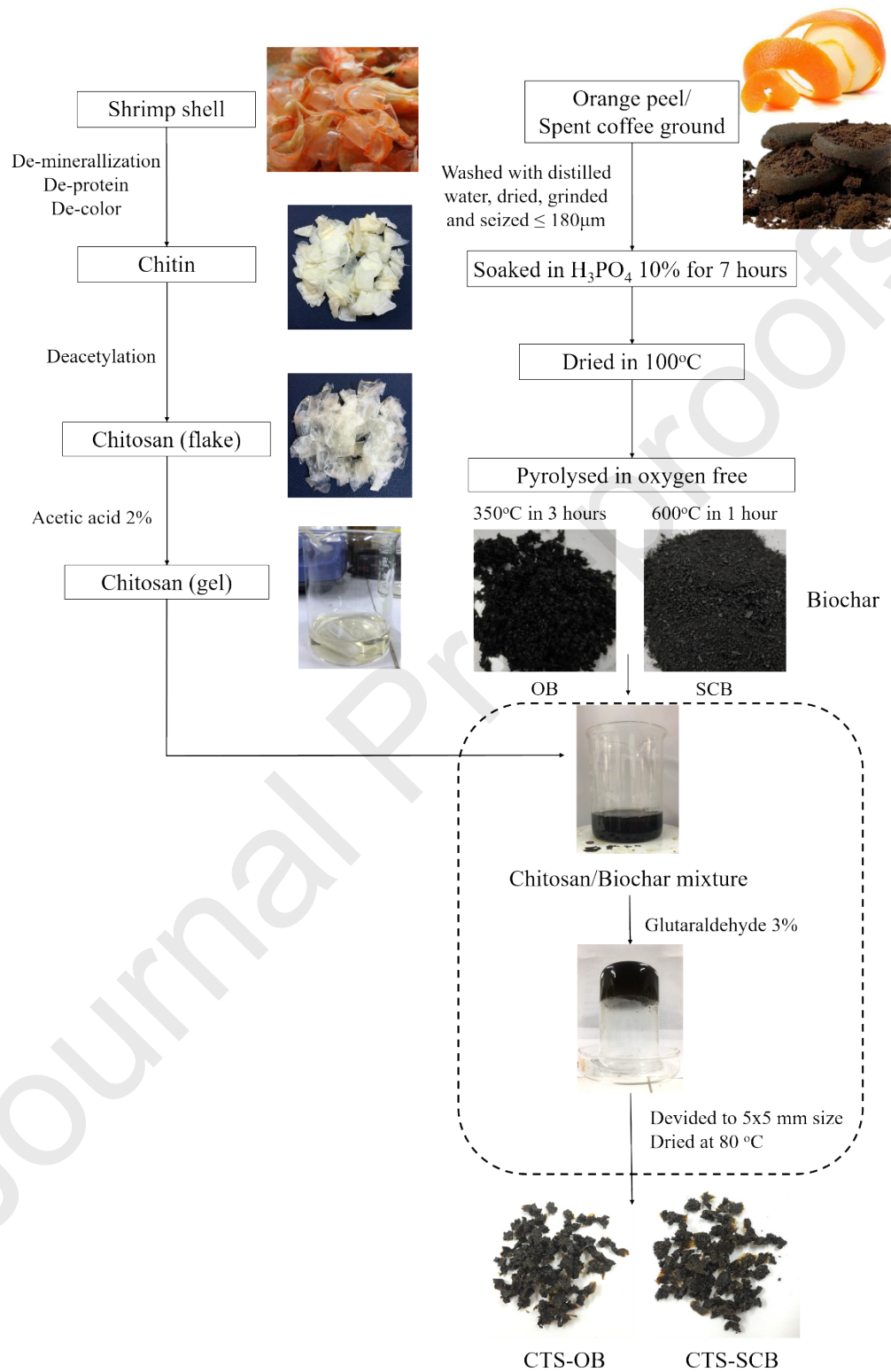


Fig. 1.

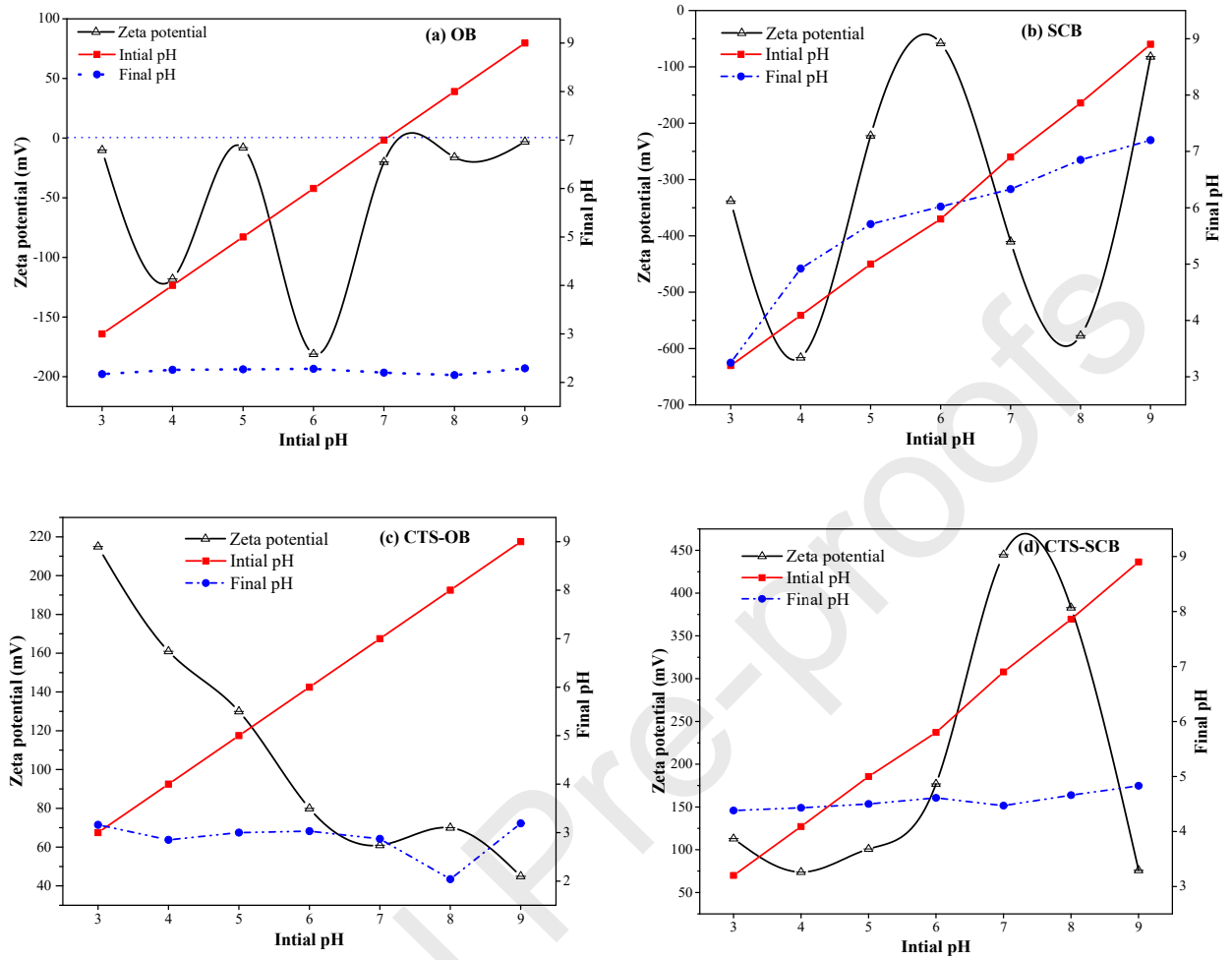


Fig. 2.

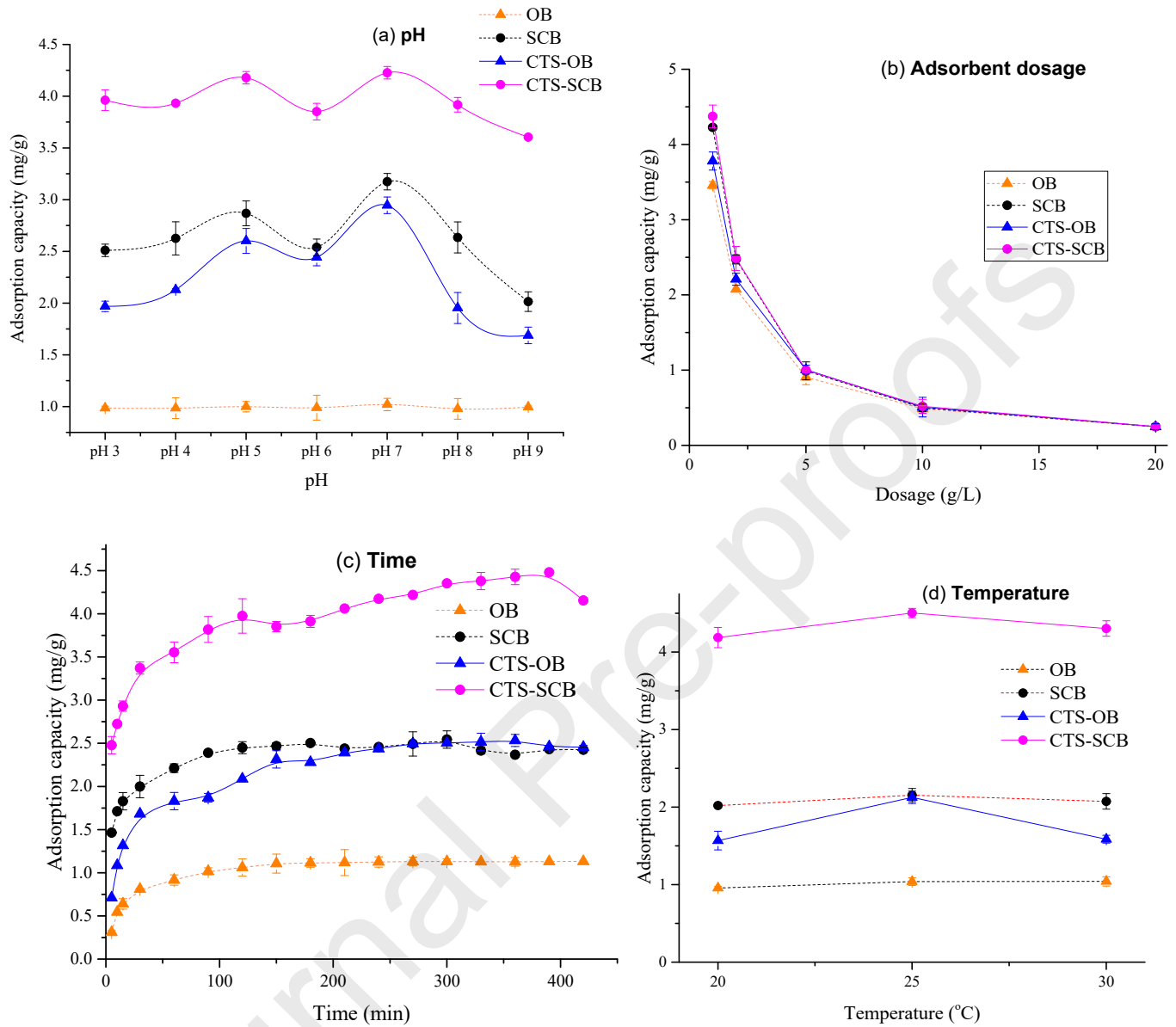


Fig. 3.

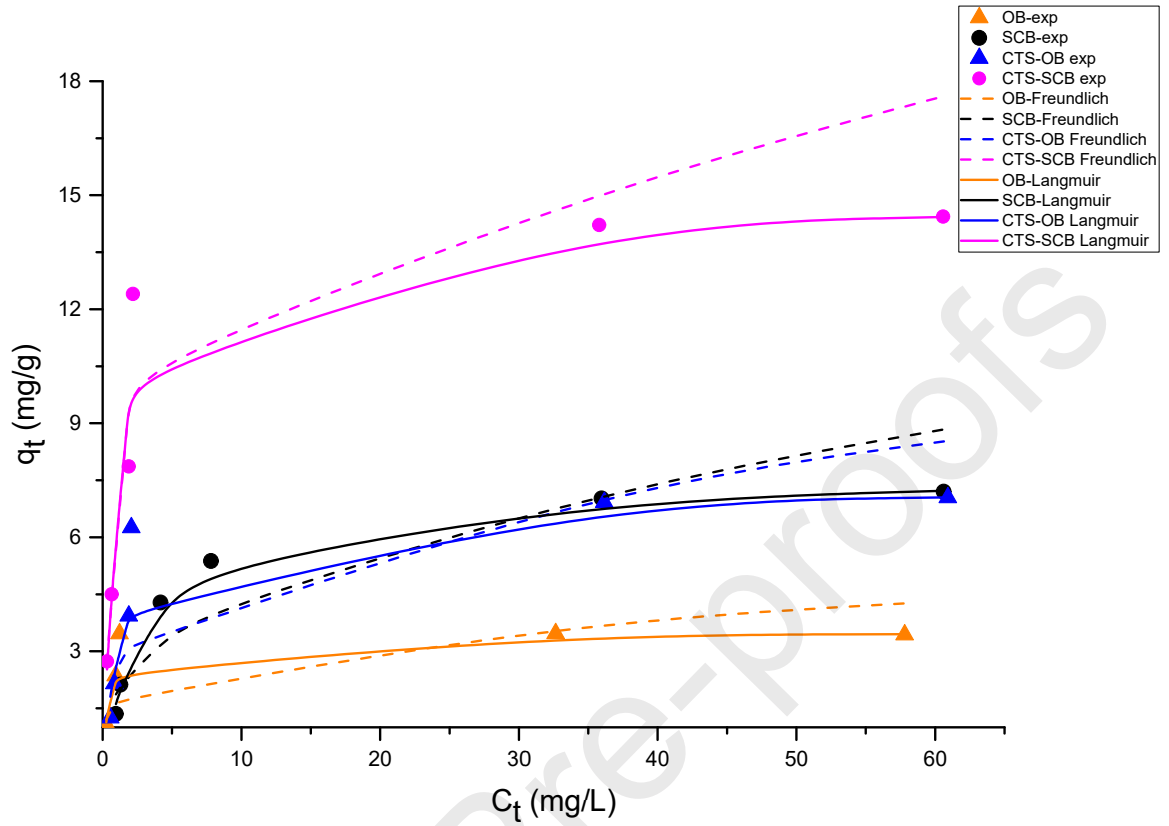


Fig. 4.

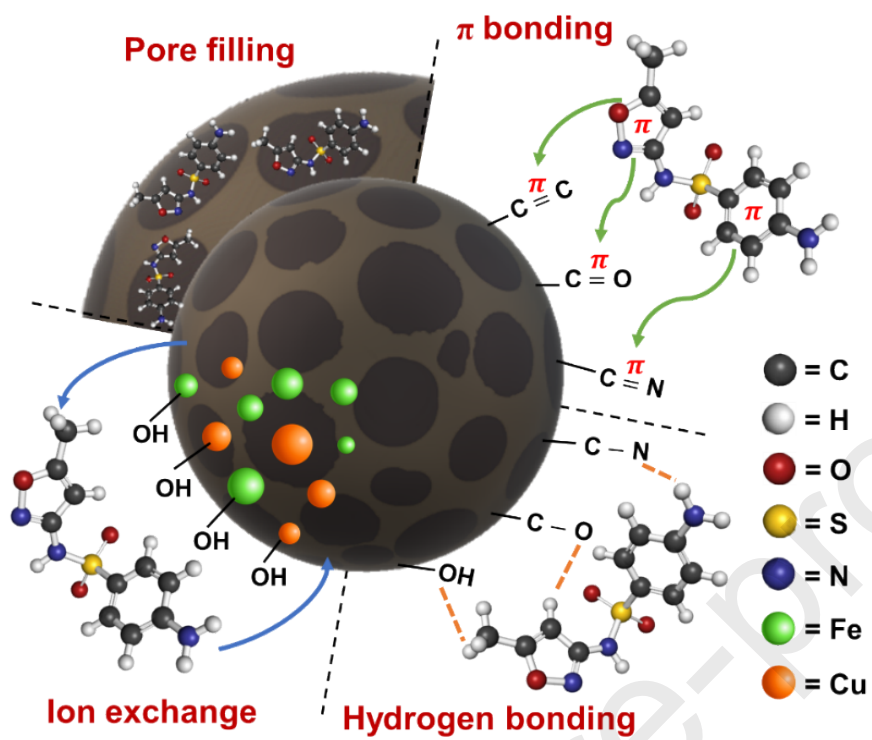


Fig. 5.